

## ■ Rationale for DD-ERS Program

### EXECUTIVE SUMMARY

#### 1. *Justification for ERS time*

Our Director’s Discretionary time for an Early Release Science (DD-ERS) program will help the community learn about the longest wavelength spectrograph on the *James Webb Space Telescope (JWST)*, the Mid-Infrared Instrument (MIRI) Medium-resolution spectrometer (MRS). We will release a suite of science-enabling products (SEPs) via a public data analysis and code repository that we have already begun to build: [github.com/miri-mrs](https://github.com/miri-mrs). The accompanying documentation is also already being written: [miri-mrs.readthedocs.io](https://miri-mrs.readthedocs.io). *Our primary SEP goal is to produce a Python package that quickly manipulates and analyzes the full MRS Level 3 data, in particular the MRS Spectral Cubes and 1D spectra.*

#### 2. *Project Management Plan & Budget*

Our team members have a long and proven history of delivering SEPs, catalogs, data products, web access pages, documentation and the necessary helpdesk support for large collaborations on strict deadlines. Our project is led by an STFC Ernest Rutherford Senior Research Fellow, who is able to contribute 100% FTE to achieving the major science goals of the proposal, as well as leading the initial development of the SEPs. We also ask for support for two postdoctoral researchers who will be in place at Launch time.

#### 3. *Scientific Justification*

Our science case is straight-forward, yet strikes at the heart of a major and still open extragalactic astrophysical question: *What are the star-formation properties of mid-infrared luminous quasars at the peak of quasar activity?* We will answer this by looking for the presence of polycyclic aromatic hydrocarbon (PAH) spectral features in  $z \approx 2.5$  infrared bright quasars. Furthermore, we will use the IFU capability of MIRI MRS in order to quantify the spatial location of the IR luminosity. This is an ideal investigation for *James Webb*; no other current or near-future facility, ground or space-based, has the combination of MIR spectroscopy, angular resolution and the sensitivity required for accessing the PAH spectral features at  $z > 2$ , *and* being able to spatially resolve their structure.

#### 4. *Description of the Targets*

We have four primary targets; all are available for early observation. We also have a back-up list of ten secondary targets, any of which would allow us to achieve our SEP and Science goals. These fourteen objects have extensive associated multiwavelength data with our four primary targets known to exhibit interesting kinematic behavior.

#### 5. *Team Diversity*

Our team is an ensemble of observational extragalactic experts with a broad geographical dispersion. This is a new collaboration, but with substantial heritage and expertise from the SDSS, the *HST/Chandra* Deep Field surveys, and more recent ground-based IR IFU collaborations (e.g., VLT/KMOS).

## Science Rationale

Over 50 years after their formal identification, and over two decades since the calculation of their space density evolution, several fundamental facts remain unknown for high-luminosity AGN, i.e. quasars: What is the main AGN triggering mechanism at the height of quasar activity at redshifts  $z = 2-3$ ? What direct observational evidence in individual objects links AGN activity to star formation? Can we observe “AGN feedback” in action, in situ, for the most luminous sources at their peak activity? Such unknowns about the co-evolution of black holes and their host galaxies remain among the most fundamental unanswered questions in extragalactic astronomy. And they will be answered with the launch of the *James Webb Space Telescope*.

Our team has identified a population of obscured, mid-infrared bright quasars at the peak of cosmological quasar activity. These sources are mid-IR luminous and may be powered by major bursts of star formation tied to an early phase of galaxy evolution/formation. However, their global star-formation properties are currently unknown. Observations with *JWST* MIRI, and in particular MRS spectroscopy, will quantify the level of star-formation in these objects. *We will observe four “extremely red” quasars with MIRI MRS across the full wavelength range to high signal to noise.* These observations will address the fundamental question of the link between star-formation and AGN activity, by quantifying and studying the morphological and kinematic properties for both of these processes; an investigation *JWST* was specifically built for.

It is unknown whether the large IR luminosities observed in these quasars is from star formation, which would produce strong polycyclic aromatic hydrocarbon (PAH) spectral features, or, if it is from the hot dust near the central quasar, which should produce much weaker/no PAH emission (due to the AGN MIR emission diluting and even destroying PAH features). *Via the detection, or otherwise, of PAH spectral features, we will measure the SFRs during what is potentially a very early/obscured stage of massive galaxy formation in the extremely red quasar population.*

MIRI MRS is the instrument of choice since no other spectrometer on *JWST* observes longward of  $5.3\mu\text{m}$ ; going redder than this is crucial in order to detect PAH features in  $z > 2$  objects. If present we will observe the most prominent, well-known major PAH emission features at  $3.3$ ,  $6.2$ ,  $7.7$ , and  $8.6\mu\text{m}$ . The mid-IR spectral region also presents a suite of high-ionization lines and critically, we will have access to the [Ne VI]  $7.65\mu\text{m}$  line which can be used to measure the instantaneous luminosity of the central engine. *The desire to immediately gain high signal-to-noise spectra in order to investigate the physics and chemistry of quasar PAHs, along with observational overhead concerns, pushes us to observe each object for 3.59 hours, for a total program Charged Time of 22.20 hours.*

## Community Access Rationale

We have already begun to design and create science-enabling products (SEPs) to help the community understand *JWST*’s capabilities. Our MIRI MRS Repo [github.com/miri-mrs](https://github.com/miri-mrs)

is active and completely accessible to anyone in the broader community. The accompanying documentation is also already being written: `miri-mrs.readthedocs.io`. *Our primary SEP goal is to produce a Python package that quickly manipulates and analyzes the full MRS Level 3 data, in particular the MRS Spectral Cubes and 1D spectra.* We note there is already Python legacy code for this type of analysis: `spectral-cube.readthedocs.io`. Critically, we have already begun working closely with the MIRI team (due to the P.I.’s location at Edinburgh) and will continue to develop tools here for the MIRI MRS.

Our timeline has delivery of the first set (‘beta’) of MIRI MRS SEPs before the Cycle 1 GO Deadline (March 2018); our v1.0.0 (with e.g. MIRSim mock data) before the launch of JWST (October 2018) and then rapid version updates once the start of science operations commences in April 2019.

Our team’s commitment to an open access ideology, not only for data, but for analysis codes, documentation, and scientific manuscripts is already evident and in place, for an example, see the P.I.’s GitHub `/github.com/d80b2t`. We are thus extremely well-placed to satisfy the overall goals of the DD ERS program.

## ■ Scientific Justification

One lasting scientific legacy of the *Hubble Space Telescope (HST)* is the discovery of massive black holes at the centers of a substantial fraction of galaxies, confirming the longstanding theory of the “central engines” of quasars. One of the major surprises from the *Hubble* was the discovery of a strong correlation between black hole mass and host galaxy properties.<sup>1</sup> This connection, causal or otherwise, may provide crucial clues to how and why these black holes formed and how their host galaxies evolved. *As of the launch of the James Webb Space Telescope (JWST), the question of how black holes affect their host galaxies is one of the outstanding questions in astrophysics.*

Observational and theoretical work now suggests that active galaxies and black holes are potentially linked to both the triggering, and “quenching”, of massive star formation. The link between massive galaxies and their central super-massive black holes (SMBHs) that appear ubiquitous is vital to the understanding of galaxy formation and evolution, and significant observational and theoretical effort has been invested in trying to measure and understand the physics involved in these systems.

The “quenching” of galaxy-wide star formation is supposedly driven by “AGN feedback”, where the AGN heats the surrounding gas corona, offsetting cooling losses and disrupting the gas inflow. This feedback manifests itself as high-velocity outflows from the AGN. *However, strong, direct observational evidence for AGN feedback is still lacking, especially for the most luminous systems at  $z = 2 - 3$ , at the height of the Quasar Epoch.* We have identified the best candidates that would possess quasar feedback in action, in situ at high-redshift. These

<sup>1</sup>Assessment of Options for Extending the Life of the Hubble Space Telescope: Final Report (2005); <https://www.nap.edu/read/11169/chapter/5>).

are the “Extremely Red Quasars” identified via their WISE W3/4 colors. As such, these mJy luminous AGN *are ideal targets for JWST MIRI*.

## The Extremely Red Quasar Population

*Extremely Red Quasars (ERQs) are a unique obscured quasar population with extreme physical conditions related to powerful outflows across the line-forming regions. These sources are the signposts of the most extreme form of quasar feedback at the peak epoch of galaxy formation, and may represent an active “blow-out” phase of quasar evolution.*

By matching the quasar catalogues of the Sloan Digital Sky Survey (SDSS) and the Baryon Oscillation Spectroscopic Survey (BOSS) to the Wide-Field Infrared Survey Explorer (WISE), Ross et al. (2015) discovered quasars with extremely red infrared-to-optical colors:  $r_{\text{AB}} - W4_{\text{Vega}} > 14$  mag, i.e.,  $F_{\nu}(22\mu\text{m})/F_{\nu}(r) \gtrsim 1000$ ; see Figure 1. These objects have infrared luminosities  $\sim 10^{47}$  erg s $^{-1}$ , and this initial study returned a heterogeneous population, spanning a wide redshift range  $0.28 < z < 4.36$ .

Hamann et al. (2017) refined the selection of the ERQs, honing the definition based on additional analysis and common properties, and found more objects in this new scheme; a core sample of 97 ERQs with nearly uniform peculiar properties selected via  $i-W3 \geq 4.6$  (AB) and  $\text{REW}(\text{C IV}) \geq 100 \text{ \AA}$  at redshifts 2.0–3.4. The core ERQs have median luminosity  $\langle \log L(\text{ergs/s}) \rangle \sim 47.1$ , sky density  $0.010 \text{ deg}^{-2}$ , surprisingly flat/blue UV spectra given their red UV-to-mid-IR colors, and common outflow signatures including BALs or BAL-like features and large C IV emission-line blueshifts. They have a suite of peculiar emission-line properties including large rest equivalent widths (REWs), unusual “wingless” line profiles, large N V/Ly $\alpha$ , N V/C IV, Si IV/C IV and other flux ratios, and very broad and blueshifted [O III]  $\lambda 5007$  (e.g., Figure 1, top right). Their SEDs (Figure 2, *left*) and line properties are inconsistent with normal quasars behind a dust reddening screen. Patchy obscuration by small dusty clouds could produce the observed UV extinctions without substantial UV reddening.

Further observations by our team with VLT/XShooter measured rest-frame optical spectra of four of the  $z \sim 2.5$  ERQs (Zakamska et al. 2016) which revealed very broad (FWHM = 2600–5000 km s $^{-1}$ ), strongly blue-shifted (by up to 1500 km s $^{-1}$ ) [O III]  $\lambda 5007 \text{ \AA}$  emission lines in these objects. In a large sample of type 2 and red quasars, [O III] kinematics are positively correlated with infrared luminosity, and the four objects in our sample are on the extreme end both in [O III] kinematics and infrared luminosity. As such, we estimate that at least 3% of the bolometric luminosity in these objects is being converted into the kinetic power of the observed wind. Photo-ionization estimates suggest that the [O III] emission might be extended on a few kpc scales, which would suggest that the extreme outflow is affecting the entire host galaxy of the quasar.

**MIR spectroscopy and PAHs:** Polycyclic Aromatic Hydrocarbons (PAHs) are abundant, ubiquitous, and dominate the structure and evolution of the ISM of galaxies. Aromatic

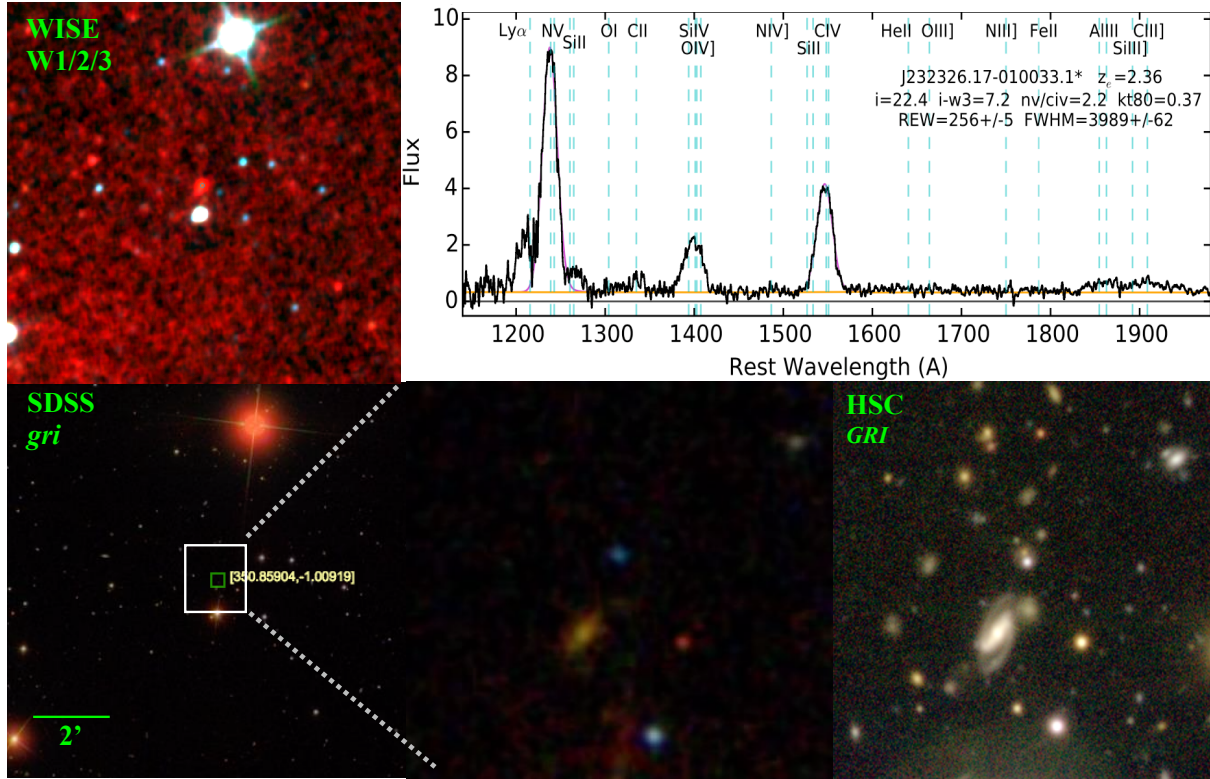


**Figure 1.** IR and optical imaging of J2323-0100, one of the four Extremely Red Quasar ERS targets. WISE (*top left*), SDSS (*bottom left*) with zoom-in (*bottom center*) and new HSC imaging (*bottom right*). The UV-rest frame spectrum (from Hamann et al. 2017) is given in the top right. Emission lines are labelled at positions marked by dashed blue lines. Note the unusual line flux ratios e.g.,  $N\,V > Ly\alpha$  and large  $N\,V/C\,IV$ . The orange and magenta curves show our fits to the continuum, and the C IV and N V emission lines, respectively. The redshift and other measured properties are also given.

features are already a significant component of dusty galaxy spectra as early as  $z \approx 2$ , and the infrared (IR) emission features at 3.3, 6.2, 7.7, 8.6, and  $11.3\,\mu\text{m}$  are generally attributed to IR fluorescence from (mainly) far-ultraviolet (FUV) pumped large PAH molecules. *As such, these features trace the FUV stellar flux and are thus a measure of star formation.* The interstellar IR emission spectrum is incredibly rich and shows a wealth of detail. It is dominated by major PAH emission features at 3.3, 6.2, 7.7 and  $8.6\,\mu\text{m}$ . In addition, there are weaker features at 3.4, 3.5, 5.25, 5.75, 6.0, 6.9 and  $7.5\,\mu\text{m}$ . *Given the redshift of our ERQs and the MIRI wavelength coverage we will cover  $1.36 \leq \lambda_{\text{emitted}} \leq 8.6\,\mu\text{m}$ .* In theory, we can detect the  $3\,\mu\text{m}$  and  $6.0\,\mu\text{m}$  water-ice feature, and figure out *where* it is most prevalent in the quasar. Figure 3 shows an example of the current state-of-the-art in quasar MIR spectral composites with  $\approx 60$  *Spitzer* IRS quasars per bin. *We will have equivalent SNR from 1 quasar, across a broader wavelength range and in a new redshift-luminosity regime.*

The mid-IR spectral region also presents a suite of high-ionization lines: [Si IX] at  $1.252\,\mu\text{m}$ , [Si X] at  $1.430\,\mu\text{m}$ , [Si XI] at  $1.932\,\mu\text{m}$ , [Si VI] at  $1.962\,\mu\text{m}$ , [Ca VIII] at  $2.321\,\mu\text{m}$ , [Si VI] at  $2.483\,\mu\text{m}$  [Si IX] at  $3.935\,\mu\text{m}$  and [Ar II] at  $6.97\,\mu\text{m}$ . However, most critically, we have access to the [Ne VI] line at  $7.65\,\mu\text{m}$ , which with an ionization potential of 158 eV is much too high for stars. **The [Ne VI]  $7.65\,\mu\text{m}$  line can be used to measure the instantaneous luminosity of the central engine.** [Ne VI]  $7.65\,\mu\text{m}$  has a critical density of  $\sim 10^6\,\text{cm}^{-3}$

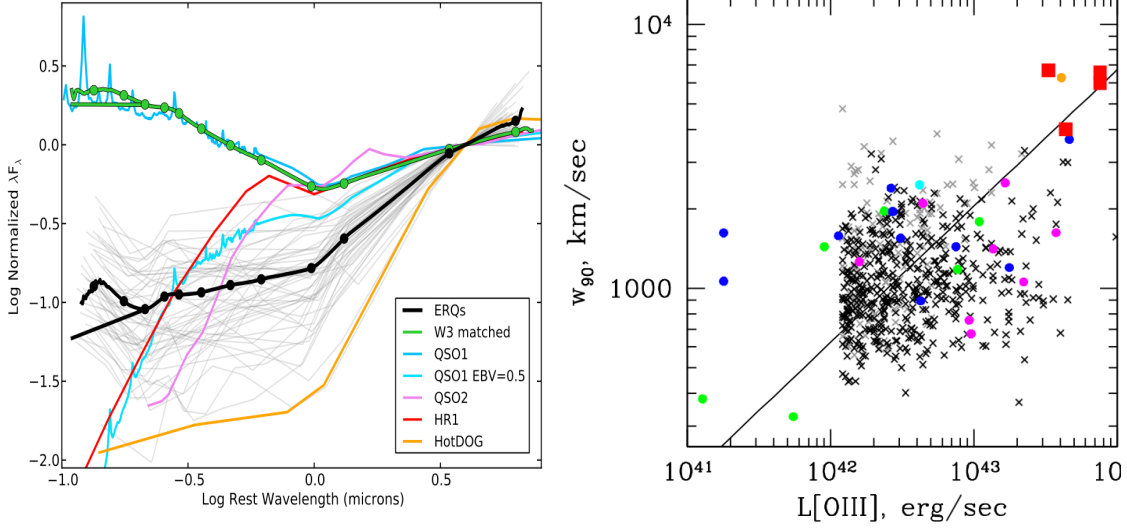


Figure 2: (Left) From Hamann et al., 2017, the normalized median SEDs for Type 1 non-BALs in the core ERQ sample (black curve) plus blue quasars matched to the core ERQs in W3 magnitude (green curve). The Type 1 quasar template with and without reddening equal to  $E(B - V) = 0.5$  (light blue, ‘QSO1’, from Polletta et al. 2007), a typical Type 2 quasar from Mateos et al. (2013; ‘QSO2’, purple), a typical heavily reddened Type 1 quasar from Banerji et al. (2013; ‘HR1’), and a typical HotDOG from Tsai et al. (2015). The light grey curves are SEDs of individual core ERQs. (Right) [O III] kinematics as a function of luminosities for our four targets, red squares, with other quasar populations are shown by black points and various colored symbols. At these extreme velocities, the gas cannot be confined by any realistic galaxy potential and is thus likely to escape from the galaxy; these objects are likely signposts of the extreme ‘blow-out’ phase of quasar feedback observed at the peak epoch of galaxy formation.

and very low interstellar extinction. Its ratio to the hydrogen recombination lines is almost independent of ionization parameter thus making this a superb emission line to utilize.

*With the IFU spatial information, at medium resolution, we will be able to (i) map the PAH emission structure of the extremely red quasars on sub-kiloparsec scales and (ii) look for offsets in these emissions that could well be indicative of ‘AGN feedback’.*

**Integral Field Unit Observations:** The ability for the MRS to obtain integral field unit spectroscopy allows us to investigate the *spatial information* associated with the high IR fluxes in the ERQs. The spatial distribution of the IR will give direct clues to the power source of the IR emission. The IFU aspect of the Medium Resolution Spectrometer will allow investigations in unprecedented detail of both the central AGN IR emission and any potentially extended emission in  $z \approx 2.5$  quasars. As a null hypothesis, we suggest that weak PAH emission will be in the nuclear regions and strong(er) PAH emission in the extended source. However, very recent studies with  $H\alpha$  of  $z \sim 2$  quasars suggest that narrow  $H\alpha$  emission might be from a spatially unresolved source.

Our final primary science goal will be to examine the IR spectral emission lines (PAH or high ionization) and place them in context with the host galaxy by looking for emission line offsets or blends. The kinematics of the [O III]  $\lambda\lambda 4959, 5007$  Å emission lines are *known to be extreme* in these objects, being very broad (FWHM=2600–5000 km s<sup>−1</sup>) and strongly blueshifted (by up to 1500 km s<sup>−1</sup>; Figure 2, right). We also know that the [O III] kinematics

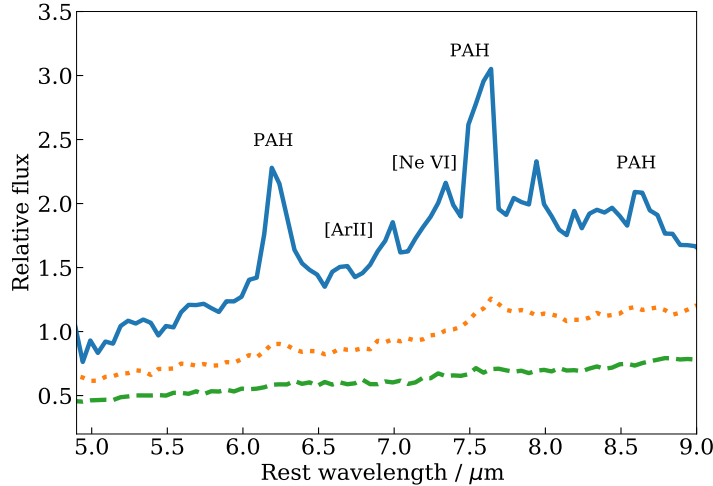


Figure 3: Example *Spitzer* IRS composite spectra, from Hill et al. (2014). Each composites has 61 quasars, in the luminosity ranges  $\log L_{5.6} = 41.0-43.6$  (blue solid),  $43.6-44.7$  (orange dotted) and  $44.8-46.1$  (green dashed). With *Spitzer* summing composites was necessary to see the spectral features; with *JWST* MIRI MRS we will be able to see these features in individual AGN. Our null hypothesis is that the dominant emission is from the AGN, but this has never been tested at our redshift or IR luminosity.

are positively correlated with infrared luminosity. Can we place the PAH and AGN emission in the same consistent kinematic structure? Is there a spatial variation of the kinematics of the IR emission lines, and if so, is it consistent with a strong ‘AGN feedback’ phase?

*Given the pixel scales of the MRS IFU, and the fact that  $1''$  is  $\approx 8$  kpc at  $z \sim 2.5$  a major challenge, goal and SEP will be to deliver software and analyses that samples the data on a sub-pixel scale.*

## Technical Description

After discussions with the MIRI Team (including European P.I., G. Wright and Instrument Scientist A. Glasse), we settled on the strategy of picking one instrument (MIRI) and one observing mode (MRS) and making sure we deliver the highest quality data analysis and SEPs in this specific instance for the community.

*Due to the nature of the ERS program, we note that we do not necessarily have to observe a full, representative sample<sup>2</sup> and given the Discretionary time available for the ERS, a natural program size is  $\lesssim 35-40$  hours.* Moreover, our program specifically tests only a particular mode of MIRI, albeit in detail, and thus our time request is curtailed in that manner. With these considerations in place, and with the desire to immediately gain high signal-to-noise spectra in order to investigate the physics and chemistry of quasar PAHs, along with observational overhead concerns, pushes us to observe four quasars, each object for 3.59 hours, for a total program Charged Time of 22.20 hours. The details of our four primary quasar targets are given in Table 1.

For our MIRI MRS operations we shall:

<sup>2</sup>Our longer term goals will be to observe a representative sample of ERQs across a range of redshifts to access e.g., the  $9.7\mu\text{m}$  silicate feature and  $11.2$ ,  $12.7$ , and  $16.4\mu\text{m}$  PAHs.

| Object Name (SDSS)               | J0834+0159     | J1232+0912     | J2215-0056     | J2323-0100     |
|----------------------------------|----------------|----------------|----------------|----------------|
| Object R.A.                      | 08:34:48.48    | 12:32:41.73    | 22:15:24.00    | 23:23:26.17    |
| object declination               | +01:59:21.1    | +09:12:09.3    | −00:56:43.8    | −01:00:33.1    |
| <i>r</i> -band AB magnitude      | 21.19±0.05     | 21.11± 0.05    | 22.27±0.12     | 21.62± 0.08    |
| WISE W4-band Vega magnitude      | 6.88±0.09      | 6.78 ±0.09     | 7.91±0.24      | 7.76±0.22      |
| WISE W4-band flux, $F_\nu$       | 14.80 mJy      | 16.23 mJy      | 5.73 mJy       | 6.58 mJy       |
| $i_{\text{AB}} - W_{3\text{AB}}$ | 6.0            | 6.8            | 6.2            | 7.2            |
| Redshift $z$                     | 2.591          | 2.381          | 2.509          | 2.356          |
| REW C IV                         | 209±6          | 225±3          | 153±5          | 256±5          |
| C IV FWHM km s <sup>−1</sup>     | 2863±65        | 4787±52        | 4280±112       | 3989±62        |
| [O III] FWHM km s <sup>−1</sup>  | 2811           | 4971           | 3057           | 2625           |
| ALMA Band 6                      | <i>pending</i> | ✓              | <i>pending</i> | ✓              |
| <i>HST</i> Cycle 24 ACS+WFC3     | obtained       | <i>pending</i> | <i>pending</i> | <i>pending</i> |
| Spectro-polarimetry              | ×              | ✓              | ✓              | ×              |
| Groups/Integrations/Exposures    | 45/1/1         | 15/3/1         | 45/1/1         | 15/3/1         |
| JWST target visibility (Start)   | 2019-04-01     | 2019-05-08     | 2019-05-22     | 2019-06-07     |
| JWST target visibility (End)     | 2019-05-07     | 2019-07-01     | 2019-07-15     | 2019-07-29     |

Table 1: Our four Extremely Red Quasar targets. All four quasars were first identified in Ross et al. (2015). Values of Rest Equivalent Widths (REW) and Full Width Half Maxima (FWHM) are from Zakamska et al. (2016) and Hamann et al. (2017).

- Operate over the full spectral coverage, and thus will use all three different spectral settings; SHORT (A), MEDIUM (B), and LONG (C).
- Use the point source optimized, “4-point ALL” dither pattern. This is the only MIRI MRS dither patterns that guarantees “GOOD” (i.e. half-integer) sampling throughout the common field of view across all four channels.
- Detector Readout mode: SLOW. Our integrations are relatively long, and the ‘Slow’ mode readout pattern offers fewer detector artifacts and slightly lower detector noise than the ‘Fast’ mode, making it a good choice for faint source medium-resolution spectroscopy where the sky backgrounds are low. This is what we want for our ERQ observations.



We are interested in only a single object per point, so no mosaicking is necessary. The Subarray is FULL (this setting is fixed for MRS).

We desire high signal-to-noise in order to *(i)* detect any low Equivalent Width PAH or AGN emission lines that might be resolved at MRS resolutions and *(ii)* immediately compare our science results to those of the *Spitzer Space Telescope* IRS studies. *With only 4 high-SNR JWST objects, we will have similar SNR as the Spitzer IRS composite studies of  $\gg 100$  objects, and at similar resolution.* Long integrations also minimize Observatory overhead, a desire that has been imparted on us by STScI operations.

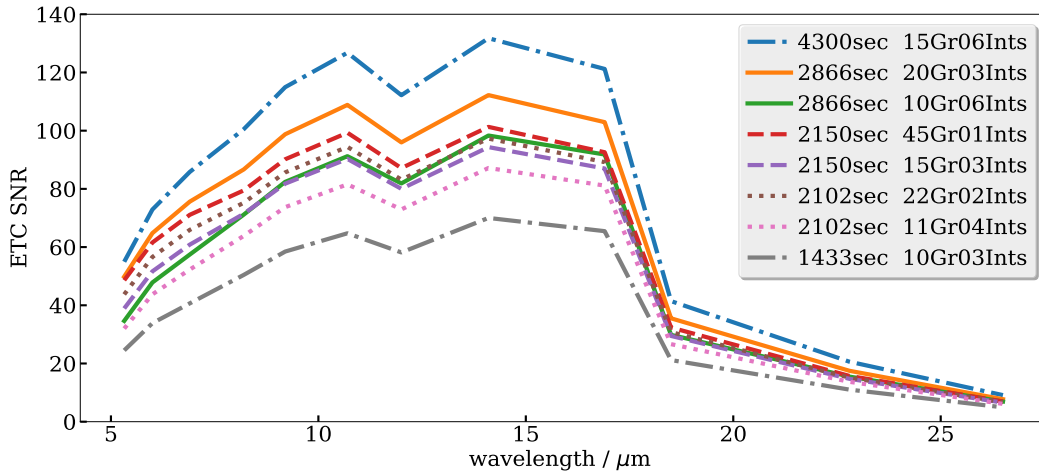


Figure 4: ETC calculations of MIRI MRS SNR values for a range of Group sizes, Integrations and the associated Science exposure time (per Wavelength disperser). The SNR is from the ETC and is per pixel. This exposure time has to be multiplied by 24 to get the full Science Exposure time: (a factor of 2 from the 2point in the ETC to 4-point dither; a factor of 3 since for all three SHORT, MEDIUM and LONG modes and a factor of 4 for the four quasars).

For the observations themselves, a wide range of considerations e.g., sample size, desired high SNR, time available for ERS programs, level of read noise, novelty of instrument, utility to the SEPs, etc., went into our estimated time calculations.

Our JWST ETC Workbook is `wb ID 7474`. In the ETC we assume the shape of the source is Point; a Medium Background; the ‘IFU Nod In Scene’; Aperture location as centered on source; an Aperture radius of 0.3”; Nod position in scene of  $X = Y = 0.5''$ . We take the “core ERQ” SED that is given in Hamann et al. (2017) and is fully representative of the ERQ population at large. The file `core_ERQ_SED_notLog.dat` is used here. We normalize this SED at a wavelength of  $23\mu\text{m}$  to a source flux density of 5mJy, again representative (and if anything on the fainter end) of the WISE W3/4-detected ERQ population and our targets. At this stage we *do not* include any emission (or absorption) lines since our null hypothesis we want to test is that the IR emission is purely from an AGN power-law.

| Object name, SDSS J | R.A. (J2000)  | Decl (J2000)  |
|---------------------|---------------|---------------|
| J000610.67+121501.2 | 00:06:10.6778 | +12:15:01.274 |
| J014111.13-031852.5 | 01:41:11.1369 | -03:18:52.567 |
| J083200.20+161500.3 | 08:32:00.2000 | +16:15:00.300 |
| J113721.46+142728.8 | 11:37:21.4663 | +14:27:28.879 |
| J121704.70+023417.1 | 12:17:04.7013 | +02:34:17.151 |
| J134254.45+093059.3 | 13:42:54.4591 | +09:30:59.396 |
| J135608.32+073017.2 | 13:56:08.3200 | +07:30:17.200 |
| J162518.66+144509.9 | 16:25:18.6600 | +14:45:09.900 |
| J215855.10-014717.9 | 21:58:55.1028 | -01:47:17.973 |
| J222307.12+085701.7 | 22:23:07.1253 | +08:57:01.735 |

Table 2: A list of Secondary targets. All of these objects will have ALMA Cycle 5 Band 6 observations. Observations of these would allow us to achieve our SEP and Science goals.

Figure 4 shows our resulting SNR values for a range of Group, Integrations and Exposures. We ultimately decided to go with two combinations of the Groups/Integrations/Exposures, for the same total Science Exposure time; see Table 1. Our final observing time request is 3.59 hours Science exposure hours per object for 14.35 Science hours total. *Using Smart Accounting, the total Charged Time is 22.20 hours.*

## ■ Plan for Alternative Targets

We have 14 ERQs that will be observed with ALMA Cycle 5, Band 6, four of which are our primary targets. The remaining 10 objects are given here as alternative targets. The redshifts and e.g. WISE W3/W4-band magnitudes and fluxes are come from the same distribution as for the core targets, hence there is no need to change the observational strategy.

## ■ Special Requirements

There are no Special Observational Requirements for our ERS.

## ■ Justify Coordinated Parallel Observations

We are not inducing Coordinated Parallels observations.

## ■ Justify Duplications

There are no duplicated observations.

## ■ Data Processing & Analysis Plan

### Summary of DD-ERS Data Products

Our primary SEP task and goal is to produce a Python package that quickly manipulates and analyzes the full MRS Level 3 data, in particular the MRS Spectral Cubes and 1D spectra. We will take the output from the third stage of the pipeline for MRS spectroscopy, the CALIFU3 level data and analyze this. We note there is already Python legacy code for this type of analysis: <https://spectral-cube.readthedocs.io/spectral-cube.readthedocs.io>.

With *a maximum* of 6 months between the first ERS observations and the Cycle 2 GO Call for Proposals, this will likely be too short for full dissemination of our findings, novel techniques and science results in the traditional manner, i.e. via published journal articles. Moreover, ongoing updated versions of our analyses and codes are envisaged to happen until right up to the Cycle 2 deadline. To solve these issues, we will fully employ the power of a code version repository system, in our case GitHub, to keep the community informed and updated with our SEPs. GitHub *has code versioning automatically built-in* so proper referencing of e.g. technical notes is straight-forward.

### Co-Investigators and Delivery of Science-Enabling Products.

All Co-Is are part of the “core team”. A team biography and SEP tasks of our team can be found [here](#) and the SEP Deliverables are [here](#). *We are acutely aware that our team currently has a gender binary split of 7:14 F:M and is predominantly White European or White American.*

### Code Repositories and Documentation

We are already ensuring open access to representative data sets, processing pipelines and analysis tools in support of the preparation of both Cycle 1 and Cycle 2 proposals. The key links are::

[github.com/d80b2t/JWST\\_ERS](https://github.com/d80b2t/JWST_ERS) (the P.I.’s public GitHub repository).

[github.com/miri-mrs](https://github.com/miri-mrs) (a “Organizational” public repository for the Community).

[miri-mrs.readthedocs.io](https://miri-mrs.readthedocs.io) (the global documentation)

### Sub-kiloparsec resolution at High-redshift

If the PAH emission from the ERQs is dominated by dusty non-nuclear star formation then we may expect it to be spatially resolved on the scale of any star-forming disk present. Typical galaxy discs at  $z = 2.5$  have half-light radii of 3 – 5kpc. The pixel scale of the MRS is 0.2-0.3” with a spatial FWHM of 0.5” (4kpc) and 0.8” (6.4kpc) for the 3.3 and 6.2 $\mu$ m lines respectively, when redshifted to  $z = 2.5$  (with the 4-point dither pattern employed). These specifications and relative sizes are very similar to those of the KMOS NIR IFU instrument on the VLT (0.2 pixel scale, median Paranal seeing 0.7). Our team has extensive experience of

analyzing star forming galaxies at  $z = 1 - 2$  with KMOS (i.e. the KROSS survey, P.I. Stott) and are therefore ideally placed to use that expertise to create post-pipeline IFU analysis tools directly analogous to those used in the KROSS survey. These will produce spatially resolved maps of PAH line strengths and velocities using the wavelength information to subsample the spatial PSF. In this way we can probe the spatial competition between the influence of star formation and the central AGN.

## **MIRISim**

MIRISim is a MIRI data simulations which includes an Integral Field observations with the Medium Resolution Spectrograph (P.I., P. Klaassen, University of Edinburgh). MIRISim does not produce final, calibrated data, instead it produces data equivalent to that straight from MIRI. We will initially concentrate on the Level 3 data cubes, but MIRISim will be a superb input for pre-Launch tests and development of the ERS ERQ SEPs that we want to develop.

## **Delivery Schedule for Science-Enabling Products**

Our ERQ ERS proposal is the first part of a multi-cycle proposal project and plan. As such, we are *already highly motivated to produce the data processing tools, codes, documentation and identify the critical science-enabling products well in advance of the release of the Cycle 2 Call for Proposals (September 2019)*. Our major milestones are::

### **Before Cycle 1 GO Proposal Deadline (end Feb 2018):**

Work with MIRI team and STScI to identify the critical MRS SEP related needs. Delivery of the first set ('beta') of MIRI MRS SEPs before the Cycle 1 GO Deadline. Write all necessary documentation scaffolding.

### **Prior to Launch (March 2018 - October 2018):**

The release of our v1.0.0, for Level 3 Data Cubes and MIRSim mock data. All documentation in place. Recruit Postdoctoral Fellows.

### **Commissioning (November 2018-April 2019):**

Full ramp-up of the Postdoctoral Fellows. Likely hold a Community workshop dedicated to post-launch, pre-science findings.

### **ERS/Cycle 1 (April 2019-September 2019):**

Rapid version updates once the start of science operations commences in April 2019. Rapid science analyses and feedback to the community. Key short technical and science papers published online.

### **After Cycle 2 GO Deadline (post-September 2019):**

Continue to provide regular (every 6 months) major version update. Key technical and science papers published in journals.

## Bibliography

Alaghband-Zadeh et al., 2016, MNRAS, 459, 999 • Alexander et al. 2005, Nature, 434, 738 • Alexander et al., 2008, AJ, 135, 1968 • Alexander et al., 2010, MNRAS, 402, 2211 • Armus et al., 2007, ApJ, 656, 148 • Banerji et al., 2015, MNRAS, 447, 3368 • Banerji et al., 2017, MNRAS, 465, 4390 • Del Moro et al., 2016, MNRAS, 456, 2105 • Fabian, 2012, ARAA 50, 455 • Cano-Diaz et al., 2012, A&A, 537, L8 • Coppin et al., 2004, MNRAS, 354, 193 • Coppin et al., 2008, MNRAS, 389, 45 • Coppin et al., 2010, ApJ, 713, 503 • Cresci et al., 2015, ApJ, 799, 82 • Daddi et al., 2007, ApJ, 670, 173 • Fu et al., 2010, ApJ, 722, 653 • Glikman et al., 2015, ApJ, 806, 218 • Hamann et al., 2017, MNRAS, 464, 3431 • Hernan-Caballero & Hatziminaoglou, 2011, MNRAS, 414, 500 • Higdon et al., 2004, PASP, 116, 975 • Hill et al., 2014, MNRAS, 438, 2317 • Kormendy & Ho, 2013, ARAA, 51, 511 • Heckman & Best, 2014, ARAA, 52, 589 • Maiolino et al. 2007, A&A, 468, 979 • Mampaso, Prieto & Sanchez, Infrared Astronomy, 2004, ISBN 9780521548106 • Mullaney et al., 2011, MNRAS, 414, 1082 • Mullaney et al., 2012, MNRAS, 419, 95 • Peeters et al, 2004, ApJ, 613, 986 • Pope et al. 2008, ApJ, 675, 1171 • Ross et al., 2013, ApJ, 773, 14 • Ross et al., 2015, MNRAS, 453, 3932 • Sajina et al., 2007, ApJ, 664, 713 • Sajina et al., 2009, ApJ, 703, 270 • Stott et al. 2013, MNRAS, 430, 1158 • Stott et al., 2016, MNRAS, 457, 1888 • Spoon et al., 2007, ApJ, 654, L49 • Tielens, 2008, ARAA, 46, 289 • Veilleux et al., 2009, arXiv:0201118v1 • Yan et al., 2005, ApJ, 628, 604 • Yan et al, 2007, ApJ, 658, 778 • Yuan & Narayan, 2014, ARAA, 52, 529 • Zakamska et al., 2016, MNRAS, 459, 3144